A report submitted in partial fulfilment of the regulations governing the award of the Degree of BSc. (Honours) Computer Science at the University of Northumbria at Newcastle

Project Report

The interplay between neonatal brain structure and function

Filip Kovarik

2023 / 2024

Declaration of Authorship

I declare the following:

(1) that the material contained in this dissertation is the end result of my own work and that due acknowledgement has been given in the bibliography and references to ALL sources be they printed, electronic or personal.

(2) the Word Count of this Dissertation is 6,860.

(3) that unless this dissertation has been confirmed as confidential, I agree to an entire electronic copy or sections of the dissertation to being placed on the eLearning Portal (Blackboard), if deemed appropriate, to allow future students the opportunity to see examples of past dissertations. I understand that if displayed on eLearning Portal it would be made available for no longer than five years and that students would be able to print off copies or download.

(4) I agree to my dissertation being submitted to a plagiarism detection service, where it will be stored in a database and compared against work submitted from this or any other School or from other institutions using the service.

In the event of the service detecting a high degree of similarity between content within the service this will be reported back to my supervisor and 2nd marker, who may decide to undertake further investigation that may ultimately lead to disciplinary actions, should instances of plagiarism be detected.

(5) I have read the Northumbria University/Engineering and Environment Policy Statement on Ethics in Research and Consultancy and I confirm that ethical issues have been considered, evaluated and appropriately addressed in this research.

SIGNED: 

Acknowledgements

I would like to express my gratitude to my project supervisor, Lucas França, for his invaluable guidance, support, and encouragement throughout this research project. His expertise and insights in computational neuroscience were instrumental in shaping the direction of my work and overcoming the numerous challenges encountered along the way.

Abstract

This project explores the connections a neonatal brain structure might have on its function and how that is linked to neurodevelopmental outcomes. It does this by leveraging convolutional neural networks (CNNs) to analyse neonatal brain magnetic resonance imaging (MRI) data. The strategy was to train a CNN algorithm to predict scores from the Quantitative Checklist for Autism in Toddlers (Q-CHAT), which provides a continuous measure of autism spectrum disorder (ASD) symptoms severity.

Initially, a 2D pre-trained CNN model was selected and adapted for 3D brain MRI data by reducing the image dimensionality. However, that resulted in the loss of spatial information and unsatisfactory performance. To address this, a custom 3D CNN architecture was developed with two convolutional layers and three fully connected layers. Despite hardware limitations restricting the model's complexity, this approach produced better results than the 2D CNN and it demonstrated the model's capability to identify discriminative features in the 3D MRI data.

The custom 3D CNN managed to achieve a mean squared error loss of 109, suggesting a connection between neonatal brain structure and neurodevelopment. The model stopped improving after this point, showing the need for more complex neural network architectures and stronger computational resources to capture the complex patterns in the brain MRI data.

This project highlights the potential of deep learning methods in neuroimaging, regardless of the challenges faced by the hardware limitations. Future work should focus on developing more advanced models, experimenting with larger dataset, and analysing functional MRI to achieve better results. Overall, this project provides a foundational step towards understanding the correlation between neonatal brain structure and function by using brain imaging and deep learning methods.

Table of Contents

Introduction

Autism spectrum disorder (ASD) is a neurodevelopmental condition characterized by difficulties in social interaction, communication challenges, and repetitive behaviours (Lord *et al.*, 2018). The ASD diagnosis is based on the observation of abnormal behaviours that may not emerge until the condition is well established, which makes timely and accurate diagnosis challenging and may prevent early and effective intervention (McCarty and Frye, 2020). Recent advancements in neuroimaging, particularly magnetic resonance imaging (MRI), have provided valuable insights into the structural and functional changes associated with ASD, introducing new non-invasive methods for early ASD diagnosis.
Structural MRI (sMRI) and functional MRI (fMRI) techniques offer detailed visualizations of brain anatomy and activity, respectively. Structural MRI enables researchers and healthcare professionals to see the physical structure of the brain and reveal abnormalities in brain regions that may correlate with ASD. Functional MRI, on the other hand, measures brain activity by detecting changes associated with blood oxygenation, highlighting how different brain regions interact during various tasks and while being at rest.

The potential of MRI in diagnosing ASD has been further enhanced by the application of machine learning techniques. Machine learning algorithms, especially artificial neural networks, have demonstrated their capabilities in pattern recognition and ASD classification tasks, making them suitable for analysing complex neuroimaging data (Rahman *et al.*, 2020). By training these models on large datasets of brain MRI images, researchers aim to develop predictive tools that can assist in the early diagnosis of ASD.

Research and Planning

Autism spectrum disorder – overview

ASD is a neurodevelopmental condition that can range from very mild to severe and affects individuals from all cultures, races, ethnicities, and socioeconomic groups. About 1 in 36 children has been identified with ASD and is almost 4 times more commonly diagnosed among boys than among girls (CDC, 2024). Although ASD individuals are diverse, they usually share core symptoms from 2 main areas – reduced social communication skills and repetitive sensory or motor behaviours (Lord *et al.*, 2018). Deficits in social communication and social interaction involve social-emotional reciprocity, nonverbal communicative behaviours, and developing, maintaining, and understanding relationships. Restricted, repetitive patterns of behaviour, interests, or activities involve stereotyped or repetitive motor movements, use of objects, or speech, insistence of sameness, inflexible adherence to routines, or ritualized patterns of verbal or nonverbal behaviour, highly restricted, fixated interests that are abnormal in intensity or focus, and hyper- or hyporeactivity to sensory input or unusual interest in sensory aspects of the environment (CDC, 2022). There is a range of screening instruments available that are designed to psychologically assess the presence of ASD in an individual. This project will focus on the Quantitative Checklist for Autism in Toddlers (Q-CHAT), which can be used to assess ASD in children. ASD diagnosis is mainly based on clinical interviews and psychological tests that observe behaviours, which can lead to misdiagnosis in children (Xu *et al.*, 2021). This creates a need to develop an objective ASD diagnosis system, which could be achieved using MRI techniques.

Magnetic resonance imaging – overview

MRI has provided scientists with means to study the living brain for which it can provide accurate pictures without the use of ionizing radiation, which is the primary negative aspect of X-rays or CT scans (Giedd, 2004). With MRI techniques, scientists can study how the brain develops throughout childhood, adolescence, and adult life. There are 2 main types of brain MRI this project will discuss. Structural MRI (sMRI), which provides anatomical images of the brain, and functional MRI (fMRI), which assesses brain function by monitoring oxygen levels in different parts of the brain.

Structural MRI

Structural magnetic resonance imaging (sMRI) is used by researchers and healthcare professionals to noninvasively study the live anatomy of the brain. The use of sMRI is popular for analysing brain morphology due to its high soft-tissue contrast sensitivity (which separates white matter, grey matter, and cerebrospinal fluid (Rafiee *et al.*, 2022)), spatial resolution, and no radiation exposure. The lack of ionizing radiation is especially important when examining children and adolescents.

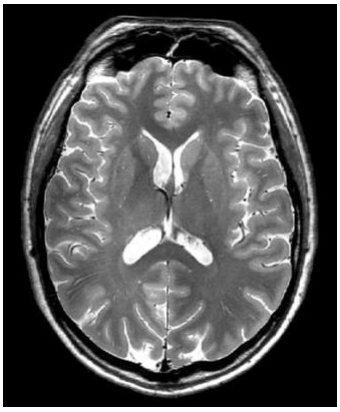

Figure 1: Brain sMRI example (Symms et al.*, 2004)*

These sMRI images allow scientists to partition the brain into different regions by defining the shape and location of each region, thus creating a brain atlas. Brain atlas mapping is a method of creating a detailed map of the brain by using biomarkers that illustrate the brain structure and function. Many of the widely-used atlases capture the architecture, function, connectivity, and topography as the four cortical properties in the parcellation (McGrath *et al.*, 2022). Several atlas-based parcellation methods analyse how different brain substructures change with age by measuring their volume (Thompson *et al.*, 2005).

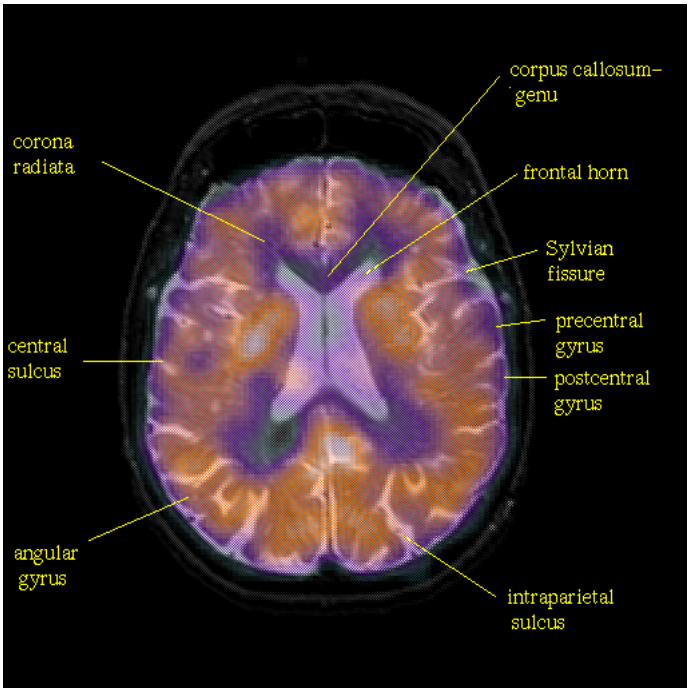

Figure 2: An example of white matter brain atlas (Johnson and Becker, 1995)

These techniques can be used to map spatial patterns of brain growth and tissue loss in children. Those are important discriminative factors for children with ASD.

Functional MRI

Functional magnetic resonance imaging (fMRI) is used to analyse the functional connectivity and activity of different brain regions. It detects neuronal activity of different brain regions

by monitoring variations in blood-oxygenation-level-dependent (BOLD) signals that respond to various forms of stimuli (Rogers *et al.*, 2007).

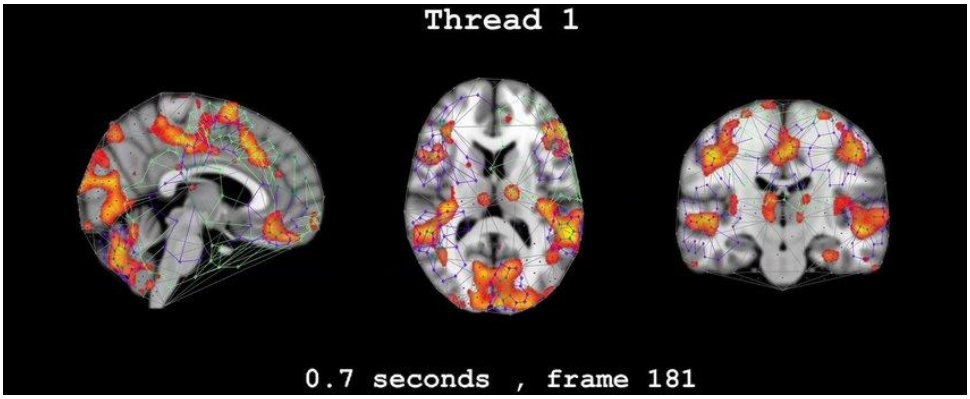

Figure 3: An example of resting-state fMRI BOLD signal vortexes on 3 brain regions (Srimal et al.*, 2019)*

When a certain region of the brain becomes more active, there is an increased demand for oxygenated blood in that area. The BOLD signal originates from hydrogen atoms, which are in the brain's water molecules. When these water molecules are exposed to a magnetic field, the hydrogen atoms absorb energy at a radio frequency that can range from tens to hundreds of MHz, depending on the type of MRI scanner used (in the case of a standard 1.5-Tesla MRI scanner, the frequency is around 64 MHz). After that, the hydrogen atoms start to emit energy at the same radio frequency until they return to their normal "equilibrium" state. The MRI scanner continuously measures the total radio frequency emitted by the hydrogen atoms. Over time, the measured signal starts to decay due to various factors, such as magnetic field irregularities. BOLD fMRI techniques focus on measuring these changes in magnetic field irregularities within small tissue volumes, which are a result of changes in blood oxygenation levels (Heeger and Ress, 2002).

Knowing which regions of the brain are active at specific points in time is important in ASD characterisation, as the brain activity shifts differently for individuals with and without ASD (França *et al.*, 2024). The downside of fMRI is its sensitivity to motion artifacts (Helmy *et al.*, 2023). This means that any movements during the screening causes a decrease in image quality.

There are two main techniques of capturing fMRI – task-based fMRI, which measures brain function while performing specific tasks, and resting-state fMRI (rs-fMRI), which analyses brain function while no specific tasks are being performed.

The application of MRI for ASD identification

Structural MRI offers multiple methods for researchers to identify and understand structural alterations in the brains of individuals with ASD (Chen, Jiao and Herskovits, 2011). Researchers agree that the brain's growth differs for individuals with ASD in the early stages of brain development. Specifically, there is an initial increase in grey matter (mental functions, memory, emotions, and movement (Mercadante and Tadi, 2024)) and white matter (nerve fibers allowing signal processing and communication between different grey matter areas (Sharma, Sekhon and Cascella, 2024)) growth during early childhood, but it is accompanied by faster synaptic pruning in early adolescence (Rafiee *et al.*, 2022). Synaptic

pruning is the removal of developing connections between brain cells (synapses) and enhancing connections supporting functional brain connectivity. During the synaptic pruning phase, individuals with more severe ASD usually experience a greater decrease in the amount of grey and white matter. Research also indicates that the rate of increased brain growth during the first year of brain development is linked to the manifestation of ASD symptoms (Rafiee *et al.*, 2022). While incorporating sMRI into ASD research has been showing consistent results in the brain's structural changes, there has been an increased focus on analysing fMRI brain scans in recent years as it was discovered that the spatial distribution of the global fMRI signal is altered for individuals with ASD, suggesting that ASD is primarily a condition of brain functional connectivity (Power *et al.*, 2017). A recent study examining brain connectivity in patients with high-functioning ASD has found that ASD is not only a matter of decreased or increased functional connectivity between brain regions, it is also a result of altered functional connectivity (Pereira *et al.*, 2018). They identified a decreased functional connectivity between the left hemisphere (speech, comprehension, arithmetic, writing (Corballis, 2014)) and posterior cingulate cortex (cognition, attention (Leech and Sharp, 2014)), and an increased functional connectivity in the right middle frontal gyrus region (numeracy (El-Baba and Schury, 2024)). Also, examining the functional connectivity strength between the right temporal pole (visual memory, face recognition (Herlin, Navarro and Dupont, 2021)) and left anterior hippocampus (episodic memory, imagination, visual scene perception (Zeidman and Maguire, 2016)), and associating that to Autism Diagnostic Interview-Revised score suggested that an increased functional connectivity in this region correlated with increased symptom severity as ASD patients with greater functional connectivity exhibited more severe social deficits.

Machine learning methods for ASD classification

Currently, ASD is diagnosed on the basis of parental/clinical interviews, behavioural observations, and using scales, such as The Autism Diagnostic Observation Schedule (ADOS) or the Quantitative Checklist for Autism in Toddlers (Q-CHAT) (Aghdam, Sharifi and Pedram, 2019; Selcuk Nogay and Adeli, 2023). It is a complicated and time-consuming process, and the use of specific scales vary among clinicians, which can lead to instances of misdiagnoses or late diagnoses. Inaccurate or late diagnosis of ASD may reduce the chances of early intervention and support. As the dispersion of ASD keeps increasing every year (Selcuk Nogay and Adeli, 2023), there is a growing need of accurate and early diagnostic of ASD. Ideally, before the manifestation of symptoms begin. One approach for addressing this is by reducing the use of traditional diagnostic techniques and developing automated and accurate systems.

The primary research focus is on employing machine learning and deep learning algorithms for ASD classification. Machine learning algorithms need large datasets for effective training. There are three primary types of data that can be used for training machine learning models on ASD classification:

- **Behavioural data** – these consist of, for example, repetitive hand flapping, body rocking, mouthing, and complex finger movements. These, and other quantitative findings collected by observing the behaviour of ASD patients, can be used for training machine learning algorithms (Nogay and Adeli, 2020).
- **Electroencephalography (EEG) data**
- **MRI data**

This project focuses on behavioural and MRI data.

There has been an increasing amount of research experimenting with various machine learning and deep learning models for ASD diagnosis after the release of popular ASD sMRI and fMRI datasets, such as Autism Brain Imaging Data Exchange (ABIDE). Abraham *et al.* (2017) extracted functionally defined brain areas from rs-fMRI and trained a support vector classification model (SVC) to compare functional brain connectivity between ASD and typically developing (TD) subjects. They trained the model on 871 subjects from the ABIDE dataset and achieved prediction accuracy of 67%. Segovia *et al.* (2014) attempted to identify the endophenotypes of autism by dividing the participants into groups of unaffected siblings of individuals with ASD, TD subjects with no family history of ASD, and subjects with ASD. They performed multi-binary classifications and studied whether siblings of subjects with ASD could be affected by ASD. They identified structural brain differences between TD subjects and unaffected siblings which they classified as possible ASD endophenotypes and argued that it could explain an increased likelihood of developing ASD symptoms for unaffected siblings of ASD individuals in later stages of their life. Katuwal *et al.* (2016) argued that the ASD classification accuracy could be improved by mitigating ASD heterogeneity. This was suggested to be achieved by incorporating autism severity, verbal IQ, and age, along with other morphometric features. They trained a Random Forest classifier on features consisting of sMRI, age, and verbal IQ of 734 males (361 ASD and 373 typically developing) and divided the subjects into sub-groups based on autism severity. They reached the highest area under curve (AUC) result of 0.92 in the low autism severity sub-group. Zhao *et al.* (2018) trained a 3D CNN on 200 subjects (ASD: 100, TD: 100) using only spatial overlap information of intrinsic connectivity network (ICN) maps and achieved an average 10-fold cross validation accuracy of 70.5%, which was substantially higher than if only ICNs without overlap information were used as input features. Jain *et al.* (2023) used Fuzzy C Means and Gaussian Mixture Model for MRI segmentation and partitioning. For feature extraction, they used Visual Geometry Group 16 networks and applied a hybrid CNN with Dwarf Mongoose optimized Residual Network, for which they achieved an ASD detection accuracy of 99.83%.

The various approaches highlighted in the literature shows the evolving nature of ML and DL models in ASD detection. Utilizing ML and DL algorithms in the analysis of behavioural and MRI data shows promise for increasing the accuracy and timeliness of ASD diagnosis. The presented examples range from sMRI brain analysis, through functional brain connectivity analysis, to the incorporation of demographic factors in classification models and showcase the growing complexity of these algorithms. In particular, the CNN and hybrid models reveal a trend of utilizing these algorithms for improved ASD detection accuracy. The current state of CNN models provides this project with a solid foundation for further experimentation and opportunity to contribute to the ongoing progress in ASD prediction through deep learning applications.

Practical Work

Design

The goal of this investigative project is to explore possible connections between neonatal brain structure and function by training a deep neural network algorithm on a dataset consisting of 3D MRI of neonatal brains. The dataset was acquired from The Developong Human Connectome Project (dHCP) (Makropoulos *et al.*, 2018) and the Q-CHAT values from CoDe Neuro Lab (Batalle *et al.*, no date). The Q-CHAT was developed to quantitatively measure autistic traits in toddlerhood. It contains a set of 25 questions, which are answered by the toddler's parent, relating to the toddler's social communication, repetitive, stereotyped, and sensory behaviours (Allison *et al.*, 2021). Each question is converted to a rating scale. The result as a single score ranging from 0 to 100, where higher scores indicate stronger autism spectrum symptoms (*Quantitative Checklist for Autism in Toddlers (Q-CHAT)*, 2008). The dataset contains a total of 782 subjects that underwent MRI and fMRI scanning withing the first few weeks after birth.

Dataset structure

The dataset provided by the dHCP has a wide range of information about all participating subjects, such as their birth age (in weeks), birth weight, sex, whether they are a singleton, etc. Each subject has their MRI scans in 2 separate folders, one contains their sMRI scan and the other their fMRI scan. Additional information for every scan session was recorded, such as the subject's age at scan (in weeks), whether they have been sedated, their head circumference, etc. Additionally, the CoDe Neuro Lab provided the Q-CHAT scores for most of these subjects. The MRI scans were usually taken within the first few weeks after birth, and the Q-CHAT assessments were conducted at 18 months of age. An example of the dataset structure can be found on the project's GitHub repository. For this project, only the following data were used for the model training:

Table 1: Example CSV data used

Subject ID	Session ID	MRI	fMRI	Q-CHAT score
sub-CC00050XX01	ses-7201	NIfTI image	NIfTI image	29
sub-CC00052XX03	ses-8300	NIfTI image	NIfTI image	35
sub-CC000112XX05	ses-37001	NIfTI image	NIfTI image	26

The MRI data are 3D brain images represented by voxel values of height, width, and depth. For viewing these images in 2D space, there are 3 different planes (orientations) available – axial (x-y plane, or from top to down), coronal (x-z plane, or from front to back), and sagittal (y-z plane, or from side to side) (Padmanaban *et al.*, 2020). Below are examples of all three planes:

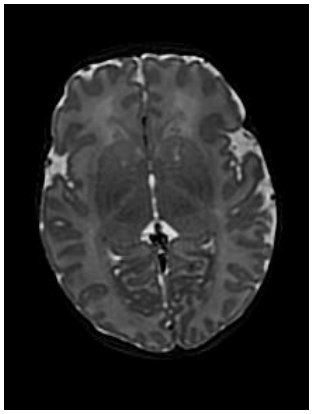

Figure 4: Brain MRI - axial plane

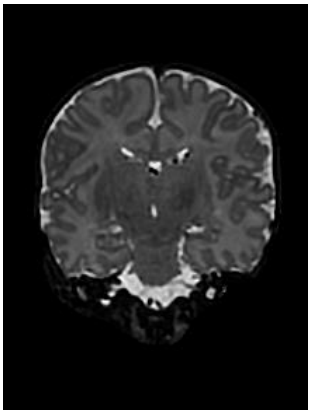

Figure 5: Brain MRI - coronal plane

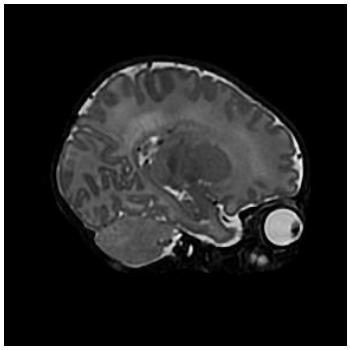

Figure 6: Brain MRI - sagittal plane

It is important to mention that the dataset contains a mix of preterm-born, term-born and postterm-born neonates, ranging from 23 weeks to 43.6 weeks of birth age. A term-born baby is considered between 39 weeks and 40 weeks and 6 days.
These are MRI examples of all three categories:

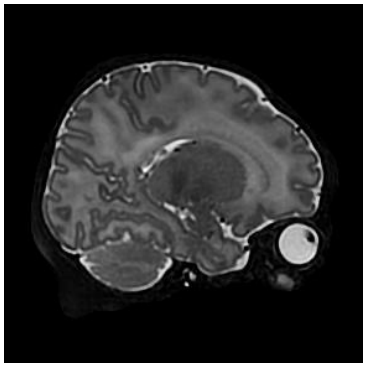

Figure 7: Term-born neonate MRI - slice 135/217, birth age: 40.3 weeks, scan age: 40.6 weeks

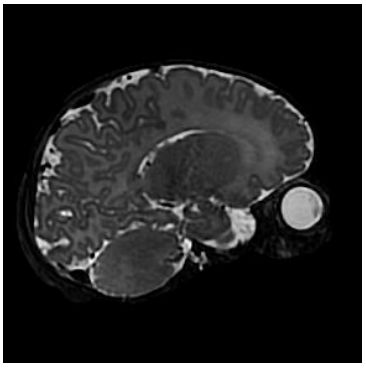

Figure 8: Postterm-born neonate MRI - slice 135/217, birth age: 43 weeks, scan age: 43.3 weeks

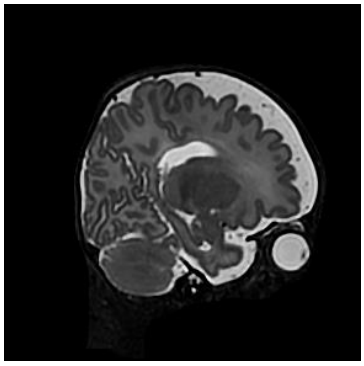

Figure 9: Preterm-born neonate MRI - slice 135/217, birth age: 23 weeks, scan age: 42.3 weeks

Hardware

As training a deep neural network model on 3D MRI images requires a powerful hardware, especially the graphics processing unit (GPU), I was assigned a high-performance computer with a GeForce GTX 970 and Ubuntu 20.04 LTS operating system installed, so I could take advantage of the CUDA cores during the training process.

Software

When deciding on the programming language for this project, the options were to use either MATLAB or Python. MATLAB offers better performance, while Python offers better community support and greater variety of libraries in the computational neuroscience field. MATLAB is a subscription-based product, while Python and its libraries are open source and free in most cases. As I wanted to make my research as accessible and available as possible

for other researchers looking to extend and build upon it, Python was the definitive choice for the project.

The PyTorch library for deep learning was selected for this project as it offers a variety of pre-trained CNN models, as well as the tools for creating custom CNN architectures. PyTorch is among the most popular open-source deep learning frameworks, along with TensorFlow and Keras. It was developed by Facebook's AI research group in 2016 and offers an easy-to-adopt package of tools for deep learning, high-performance for training on large datasets, GPU acceleration for faster model training, a variety of pretrained models, and a strong community of neuroscientists using PyTorch for their research (Pykes, 2023). TensorFlow has better corporate backing and excels in its accessibility across multiple platforms, such as CPUs, GPUs, TPUs, or mobile devices, compatibility with several programming languages, such as Python, C++, or Java, and scalability. On the other hand, TensorFlow is reportedly more difficult to debug than PyTorch or Keras, and has a more complex architecture then its competitors, making it more difficult to learn and adopt (Zafar, 2023). Keras provides a simple, user-friendly API, which allows developers to rapidly build models with a few lines of code, but is designed for smaller models and datasets, which does not make it a good candidate for training complex models on large MRI datasets.
Other libraries used for this project include:

- NiBabel – a library for reading and writing neuroimaging data, used in the script for loading MRI data in NIfTI file format,
- NumPy – a library for numerical computations, used in the script for array manipulations and data transformations,
- Pandas – a data manipulation and analysis library, used in the script for reading a CSV file containing file paths and MRI data labels,
- scikit-image – used in the script for downsampling the MRI images to a specified size,
- torchvision – a library for computer vision tasks, used in the script for reading images, applying transformations, and accessing pre-trained models.

The data preprocessing part involved creating a CSV file that would be used in the script to create and initialize the dataset for the model. I used a Bash script for generating a CSV file with a list of folder and file names that I could use to access and read the MRI images (Anderson, no date). As the MRI and Q-CHAT data came from 2 separate sources, I had to merge the 2 lists to ensure all the subjects were assigned the correct Q-CHAT scores. Additionally, some of the Q-CHAT scores were empty or had a value of -999, so I removed those rows from the dataset. This reduced the number of samples from 782 to 592.

To familiarize myself with the 3D MRI structure, I used FreeSurfer, which is a neuroimaging toolkit for processing, analysing, and visualizing human brain MRI (*FreeSurfer*, no date).

Methodology

The goal of this project was to find if the brain's function is influenced by its structure by using a CNN. I aimed to achieve this by training a CNN model on the structural MRI. The hypothesis was that if the model would be able to learn from the dataset and improve its performance over time, it would indicate a connection between the brain's structure and function.

As there are no pre-trained 3D CNN models for PyTorch, I used a pre-trained 2D CNN model and adapted the data to fit the architecture. As the model's performance was not satisfactory (further explained in the investigation chapter), I eventually decided to create my own 3D CNN architecture. The 3D structural MRI images are of size [217, 290, 290]. To accommodate for hardware that was available to me, the images needed to be downsampled. I used an average pooling filter to downsample the MRI images to [109, 145, 145]. The CNN architecture illustrated below:

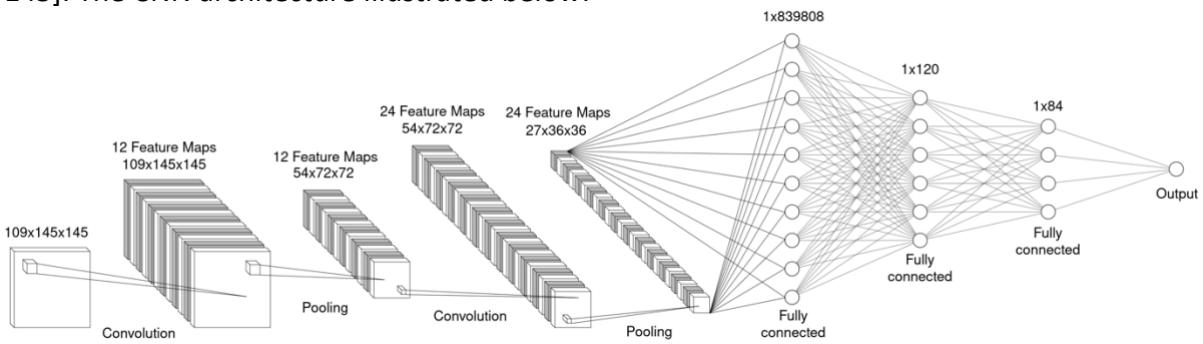

Figure 10: CNN architecture diagram (the number of neurons displayed in the fully connected layers is reduced to fit the diagram)

The feature extraction part contains 2 transformation sequences:

- The first sequence reads a [109, 145, 145] MRI image and applies convolution using 12 filters of size 3x3x3 to produce 12 feature maps of size 109x145x145. A zero-padding is also applied around the edges to preserve the image dimensions. After that, a max-pooling filter of size 2x2x2 is applied to downsample each feature map to 54x72x72.
- The second sequence uses the same technique, taking the 12 feature maps as input, applying convolutional filters to produce 24 feature maps. A max-pooling filter is then applied to further downsample the feature maps to 27x36x36.

The extracted features are then flattened into a 1D array of 839808 elements and used to create a fully connected neural network with 3 layers. The output uses a rectified linear unit (ReLU) activation function, which normalizes the predicted values between 0 and 1. This creates the need to scale the output, so it corresponds to the predicted Q-CHAT scores. The dataset was split into a training set (70% of the dataset), validation set (15% of the dataset), and testing set (15% of the dataset). The CNN model was loaded with the training dataset of MRI images and their corresponding Q-CHAT scores. Using the validation dataset, the training loop was configured to stop running after the fifth occurrence, where the model stops improving.

The training loop reads an MRI image, predicts a Q-CHAT score, calculates the loss using mean-squared error, and performs backpropagation to update the parameters (weights and biases). After each training epoch, there is a validation loop which compares the current epoch's average loss to the previous best average loss on the validation dataset. After the training is finished, there is a testing loop which predicts Q-CHAT scores on the testing dataset and calculates the average loss, which is used to determine the model's performance.

The project files and the code can be found here:
https://github.com/AlgosL/q-chat_cnn

Analysis

The model's performance is measured at 3 separate points in the pipeline. During the training loop, the average loss after each epoch is calculated using mean-squared error. After each epoch, there is a validation loop that calculates the current average loss for the validation dataset. After the training is finished, there is a testing loop that predicts Q-CHAT scores for the testing dataset and calculates the average loss, which is used as a measure of the model's performance. The goal is to train the model to understand structural differences in the neonatal brain to be able to predict Q-CHAT scores, which are measured at 18 months of age.

Ethical and safety guidelines

The dataset was acquired by the dHCP. This dataset is public and the study was conducted to the principles of the Declaration of Helsinki ('WMA - The World Medical Association-WMA Declaration of Helsinki – Ethical Principles for Medical Research Involving Human Subjects', no date). Additionally, all data are stored on the University's OneDrive network and where appropriate additionally protected with a password. Occasionally some results might be presented at a conference or published in a journal, but they will always remain anonymous. All data used in this project will be secondary data and will be stored in line with the General Data Protection Regulation (GDPR).

Investigation

This chapter is dedicated to describing the challenges that arose during the project in more detail and explaining the steps taken to address them. As previously explained in the methodology chapter, the initial strategy was to use a pre-trained 2D CNN model for simplicity and feasibility. However, a custom 3D CNN architecture was developed later due to a lacking performance of the pre-trained 2D CNN model. First, I will describe the challenges with the pre-trained 2D CNN model before moving on to the custom 3D CNN model.

The pre-trained 2D CNN model I decided to use was one from the PyTorch's repository – ResNet. ResNet is a pre-trained CNN model for image recognition (*ResNet*, no date). It was trained on the ImageNet, a visual database designed for object recognition in images that contains more than 14 million annotated pictures (*ImageNet*, no date). As the architecture of the pre-trained ResNet model is designed for 2D images, I had to reduce the dimensions of the 3D brain MRI. The ResNet model accepts a 4D tensor of shape [batches, channels, height, width]. To solve this problem, I sliced the 3D images along the x-axis, which transformed them into 2D images, corresponding to the sagittal plane view. This resulted in each subject having 217 2D images of size 290x290 (the original size was 217x290x290). After that, I created a tensor from these images and inserted the slices into the batch dimension, resulting in a tensor of size [217, 1, 290, 290].

This introduced a hardware requirement issue as suddenly for a dataset of 592 subjects I had 128,464 images in total. I was not able to train the model due to the GPU memory limitations, so I had to reduce the number of slices from 217 to 21. This resulted in a loss of spatial information from the images, but it allowed me to train the model on the available hardware. However, the model did not perform well and showed signs of overfitting. After further experimentation, I decided to create a custom 3D CNN architecture to solve the overfitting and spatial information loss problem. However, to be able to train the model on the available hardware, I had to simplify the model's architecture (Figure 10) and reduce the resolution of the 3D brain MRI to 109x145x145 by applying a 2x2x2 average-pooling filter.

Results

For comparison, I am including the performance measures for my initial pre-trained 2D CNN and the custom 3D CNN architecture. The loss value is measured using a mean-squared error (MSE) function, which is defined by the following formula:

$$MSE = \frac{1}{N}\sum_{i=1}^{N}(y_i - \hat{y}_i)^2$$

Where:

- N is the batch size (number of samples being tested against),
- y_i is the tensor of target values for the i-th sample,
- $\hat{y}$ is tensor of predictions for the i-th sample.

The MSE, or L2 loss, is a function that quantifies the size of the error made by a machine learning model by calculating the average/mean of the squared differences between the model's predictions and the actual (ground truth) values. By squaring these differences, the MSE gives a greater penalty to larger errors, meaning that the model is more penalized for predictions made far off from the correct value. The process of averaging these squared errors across the predictions normalizes the total errors against the number of samples in the dataset or batch (Wang and Bovik, 2009).

Comparing the training loss between the pre-trained 2D CNN and the custom 3D CNN, the pre-trained 2D CNN model's loss value stops showing significant improvements after the second epoch and stabilizes on a value of around 100 (Figure 11). On the other hand, the custom 3D CNN model shows a more complex learning curve than the pre-trained 2D CNN model. The loss is larger at the beginning and decreases by a larger margin for the first 2 epochs than for the other epochs. This can be explained by the complex nature of the training data, which involves a great number of features for the model to learn from. The model then continues to learn, gradually reducing the training loss until around epoch 21, where the model stops improving, therefore early stopping is triggered a few epochs later. There is also a temporary spike of training loss at epoch 7, which could be due to several reasons. Most notably, if the learning rate was too high for that epoch due to rate scheduler adjustments, it might cause the model to overshoot the optimal point. A few other potential reasons might be batch variability (the training data could have been more complex or unique), or the model adjusting to regularization (dropout layer). Even though the loss value

was always lower for the pre-trained 2D CNN model compared to the 3D CNN model, this does not result in the pre-trained 2D CNN model performing better. The model's inability to minimise loss after the second epoch suggests that the model was not able to determine many discriminative features from the training data. This is further supported by comparing the validation losses between the two models, where the pre-trained 2D CNN model did not perform well (Figure 12). This means that the model struggles with predictions on unseen data. This is likely due to the lack of spatial information from reducing the dimensions and resolution of the MRI images. The complete training data are listed in the appendices (Appendix 3-5).

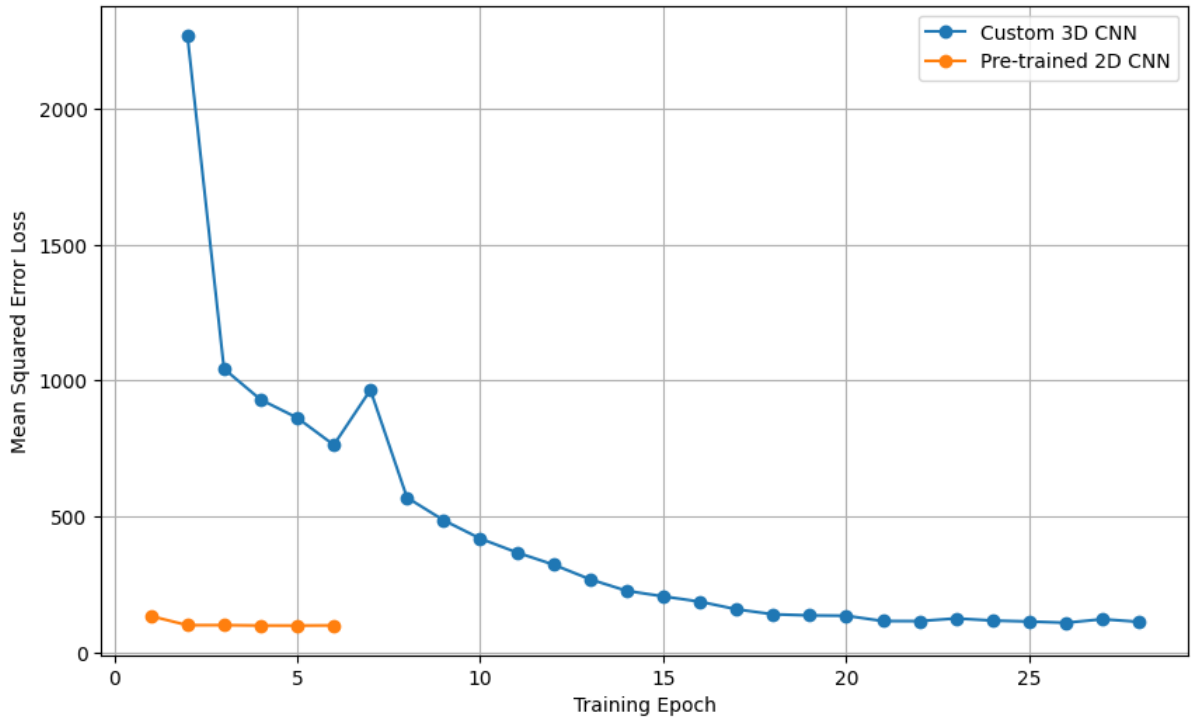

Figure 11: Comparing training loss between the pre-trained 2D CNN model and the custom 3D CNN model. The first epoch's loss is not displayed for the 3D CNN to fit the graph.

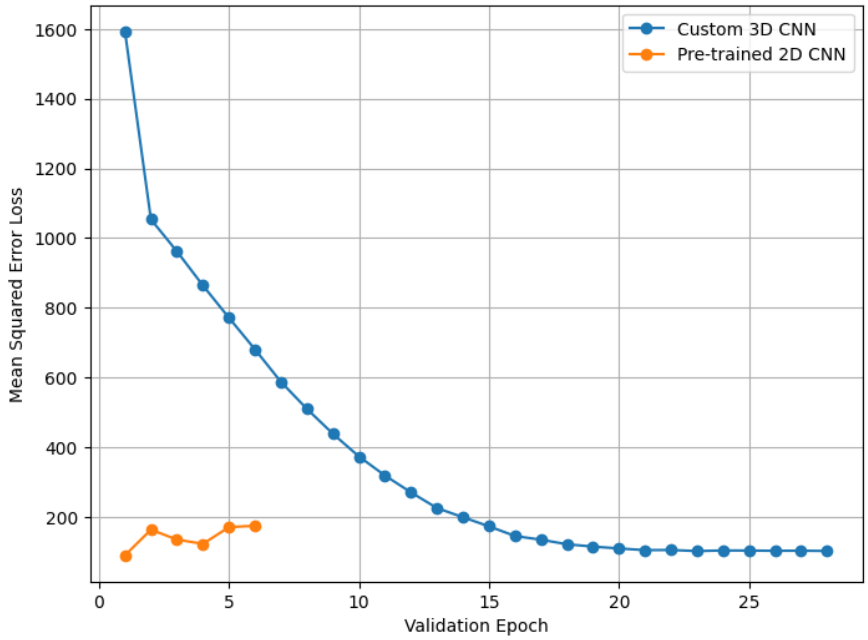

Figure 12: Comparing validation loss between the pre-trained 2D CNN model and the custom 3D CNN model

Using the testing data, the loss for the pre-trained 2D CNN model resulted in 238.58 while the loss for the custom 3D CNN model resulted in 77.458. This further supports the need of preserving as much spatial information as possible from the images that the model can learn from.

Evaluation

The results from the 3D CNN model's performance show promise in indicating that the model can extrapolate relevant features from the brain's structure that determine the Q-CHAT results. The root mean square deviation (RMSD) calculation can be applied to determine by how much the model's predicted values are off from the ground truth values on average. Below is the equation for calculating RMSD:

$$RMSD = \sqrt{MSE} = \sqrt{\frac{\sum_{i=1}^{N}(y_i - \hat{y}_i)^2}{N}}$$

The loss value of 77.458 on the testing data means that the difference between the ground truth values and the model's predicted values was, on average, 8.8. This arguably indicates a good performance considering the Q-CHAT scores range from 0-100 and could support the hypothesis that the brain functions could be influenced by its physical structure. However, analysing the dataset in more detail might challenge the previous statement. The dataset contains 592 subjects, each having an MRI scan after birth and a Q-CHAT assessed at 18 months of age. For the model to be able to train well on this regression task, it needs a good amount of data representing the whole scale of possible Q-CHAT scores. I have divided the dataset into groups by their Q-CHAT values and counted the distribution of subjects for each group. The bar chart below shows the distribution of all Q-CHAT scores in the dataset. It shows that the most amount of data is centred around the 21-30 category, very few samples are available for the 0-10 category, and no samples with Q-CHAT scores above 70 are present.

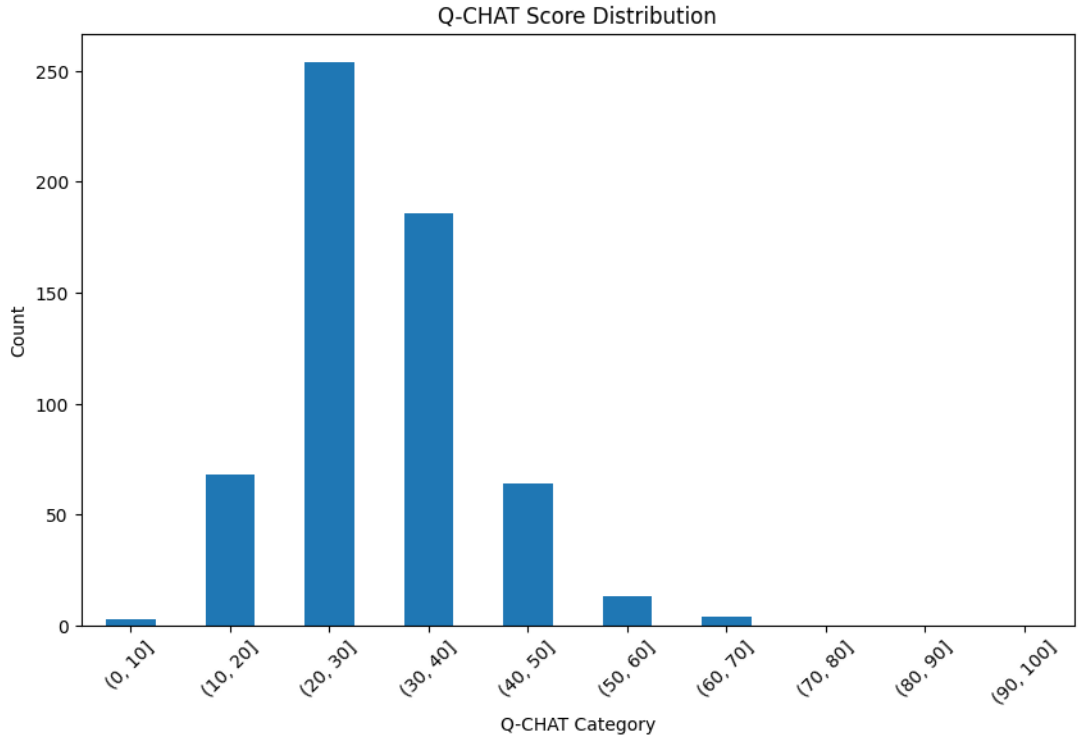

Figure 13: Q-CHAT score distribution in the dataset

This creates an issue as there is a strong likelihood the model is biased towards predicting values in the range where most of the samples lie. This is because the model's primary goal is to minimize loss, which it can achieve by predicting values in the densest range of Q-CHAT scores. In this case, the MSE performance metric might not reflect the true performance of the model as the model might not perform well on unseen data in the less represented ranges.

To address this issue, I decided to oversample the underrepresented Q-CHAT ranges for the training dataset. I assigned a weight to each Q-CHAT score value in the dataset based on how many times that score occurs in the dataset, giving higher weight to underrepresented scores and lower weight to overrepresented scores. After that, I apply an algorithm that uses the weights as a probability metric for choosing data samples for the training dataset. In other words, the underrepresented samples are more likely to be included in the training dataset and they can also be drawn more than once. This strategy resulted in the following distribution for the training dataset.

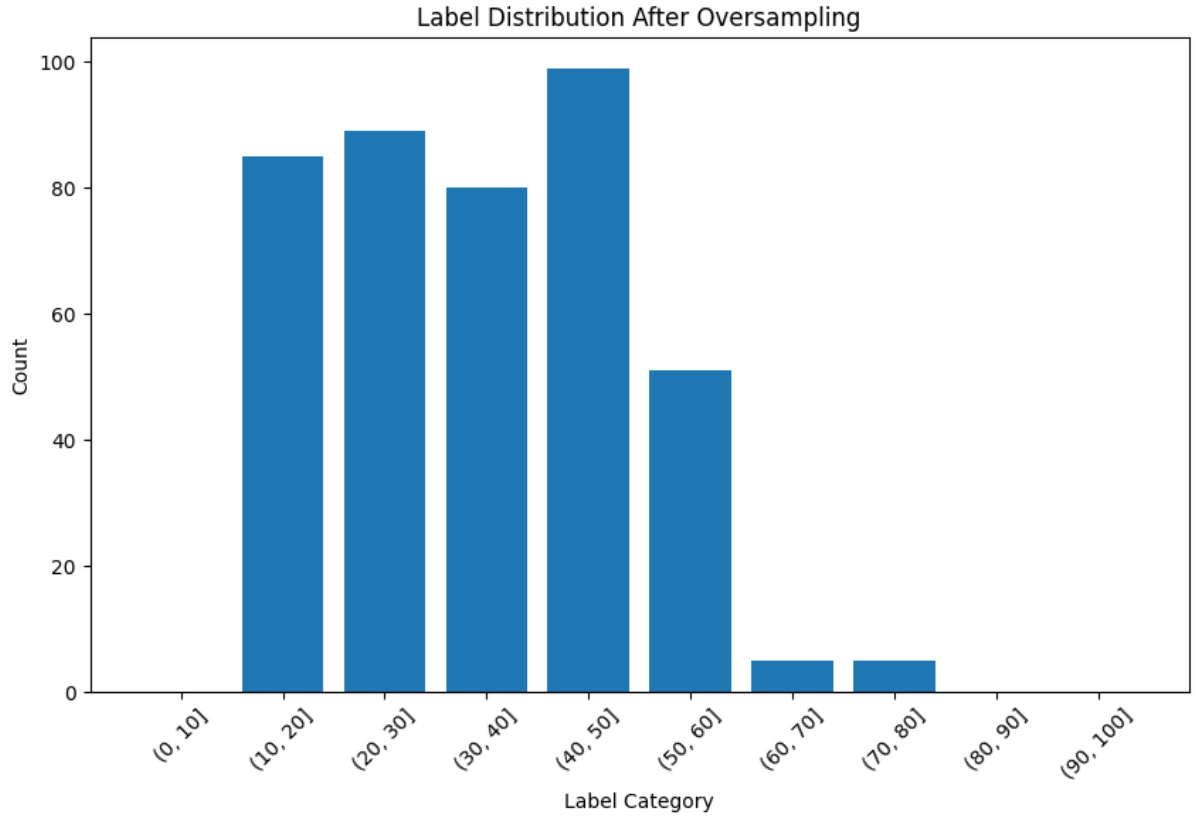

Figure 14: Q-CHAT score distribution in the training dataset (70% of the whole dataset) after oversampling

This significantly reduces the risk of having a biased model, as now the dataset is distributed more evenly, and the model does not focus just on a specific Q-CHAT range to minimise loss. The results after retraining the model indicate that the model remains capable of learning the patterns from the MRI images and minimise error. The training loss develops in a similar fashion as before, but the validation loss struggled to improve at epochs 5, 9, 20, 24, and 28. For the rest of the epochs, the validation loss was decreasing steadily until around 114,

which is likely the limit of the simple CNN architecture. The average loss for the testing dataset was 109. These results suggest that there is a connection between the neonatal brain structure and function, and that relevant features from the brain structure could be used for early identification of neurodevelopmental outcomes.

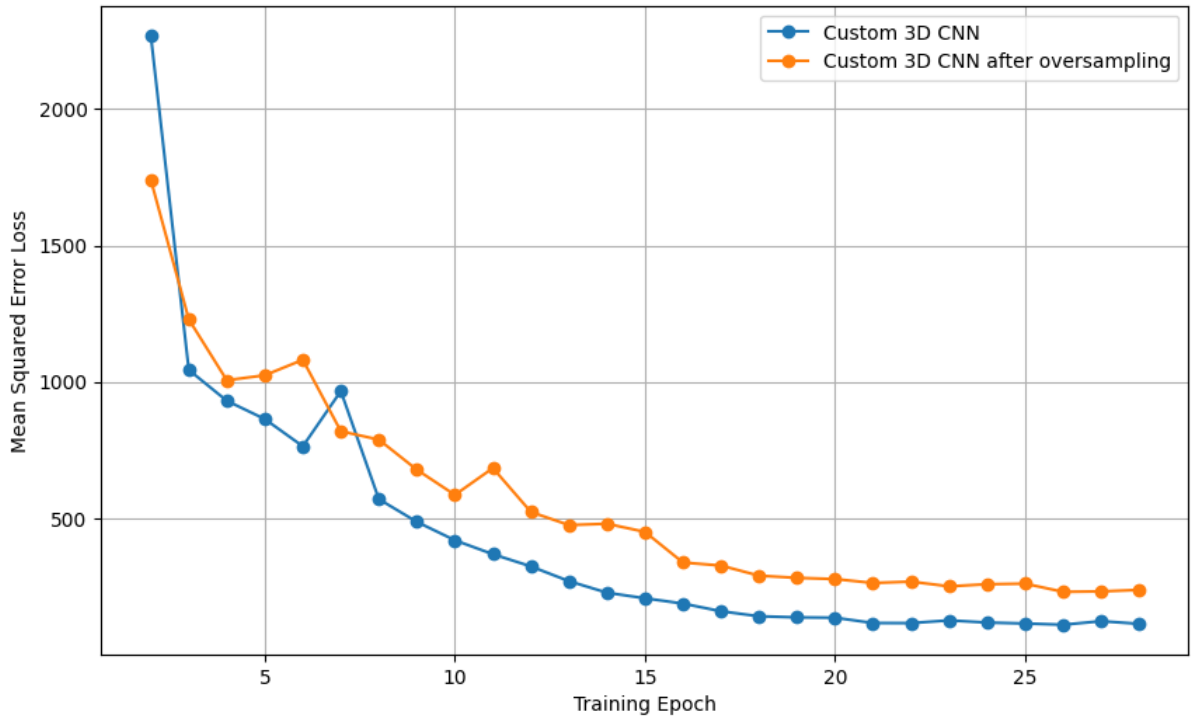

Figure 15: Comparing training loss of the custom 3D CNN model after dataset oversampling was applied against the previous custom 3D CNN model. The first epoch's loss for both models is not displayed to fit the graph.

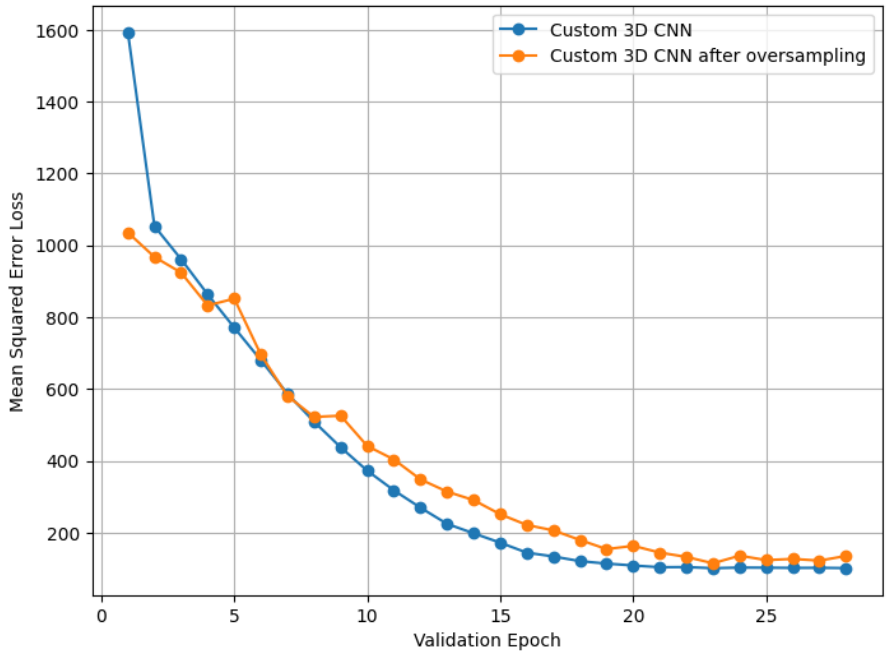

Figure 16: Comparing validation loss of the custom 3D CNN model after dataset oversampling was applied against the previous custom 3D CNN model

Evaluation of the project process

This project allowed me to analyse neonatal brain MRI data acquired within the first few weeks after birth. The dataset was made available to the research community in 2022 by the dHCP with a goal to provide researchers with means to investigate typical and atypical brain development across the perinatal period (Edwards *et al.*, 2022). ASD symptoms can be identified as early as 18 months of age, but a reliable diagnosis by an experienced professional is usually made by the age of 2 (Okoye *et al.*, 2023). By having access to the dataset of neonatal brain scans and the Q-CHAT assessment scores, which are conducted at 18 months of age, I applied deep learning methods to analyse and identify structural changes in the brains of neonates that would indicate the results of the Q-CHAT assessment. If successful, this would have the potential to support further research and help identify ASD biomarkers, as well as other neurodevelopmental outcomes, within the first few weeks after birth. This task was both ambitious and challenging due to the neurodevelopmental changes that occur in the brain during this period and the subtle nature of early biomarkers of ASD.

This project also required me to acquire new skills in computational neuroscience and Python and its relevant libraries for handling brain MRI images and deep learning. The primary objective of the project was to investigate possible patterns of how the neonatal brain structure might be linked to its function by applying the principles of deep learning to analyse 3D brain MRI images and then extend that to include the 4D fMRI images as well. However, constraints in terms of available time and hardware resources have not allowed me to realize the latter goal. Despite these challenges, the project provided valuable insights into the application of deep learning for investigating connections between the neonatal brain's structure and function.

The initial stages of the project were dedicated to familiarizing myself with Python and all the libraries that were needed for analysing brain MRI images, implementing deep learning algorithms, and structuring the data to fit the model. This knowledge was needed for later experimentation with various pre-trained 2D CNN models, and eventually, for the development and training of my own 3D CNN model.

One of the critical challenges faced during the project that was discovered late in the process was the uneven distribution of data within the dataset. This issue led to a bias in the model towards the more represented label ranges, which affected the overall accuracy and reliability of the model's predictions. Reflecting on this experience, it is clear that a thorough analysis of the dataset prior to the model training would have been useful in identifying and addressing potential biases and other issues early in the project.

This project has enhanced my skills in analysing brain MRI images in Python, data processing, and applying machine learning methods to medical problems. I have acquired new knowledge of medical image data transforms and oversampling, designing a custom CNN architecture tailored to specific data types while balancing model complexity and computational feasibility, and applying/interpreting continuous performance assessment metrics, such as MSE. The experience also highlighted the necessity of careful data analysis and preprocessing in the development of deep learning models. Moving forward, I plan to

incorporate the insights and knowledge I gained into future projects to ensure a more robust and accurate model training pipeline.

Conclusion and Recommendations

This project investigated the interplay between neonatal brain structure and function by applying deep learning techniques on neonatal brain MRI. The aim of the project was to investigate these possible patterns by training a machine learning model. For simplicity, I initially employed a 2D pre-trained CNN model from the PyTorch repository and adapted the 3D brain MRI to fit the model by reducing the images dimensionality. This preprocessing step resulted in a loss of spatial information, limiting the model's ability to effectively learn from the data. To address the limitations of this approach, I designed a custom 3D CNN architecture capable of processing the 3D MRI data. Due to hardware limitations, this model only consisted of two convolutional layers and three fully connected layers. Despite its simplicity, this architecture showed improved performance over the pre-trained 2D CNN model. The custom 3D CNN model managed to capture some discriminative features from the MRI images, which is demonstrated by its ability to minimise loss on predicting Q-CHAT scores to a certain extent. However, the model stopped improving after a certain point, stabilising on an MSE loss of around 114.
Despite the challenges posed by the limited research on this topic and hardware limitations, this investigation has provided valuable insights. By training a custom 3D CNN on brain MRI, albeit with a relatively simple architecture design, I have shown that it is possible to extract meaningful discriminative features from neonatal brain MRI data that correlate with relevant neurodevelopmental outcomes.

Recommendations for Future Work

The ability to predict Q-CHAT scores from neonatal brain MRI opens new possibilities for early detection and intervention of ASD in toddlers. This could lead to earlier support for children who may be affected and could potentially help positively influence the course of their development. However, there is still room for improvement for this project. Future research could explore more sophisticated CNN architectures, different deep learning algorithms, or even ensemble methods to improve the prediction accuracy. Below are suggestions for improvements and extensions:

- **Increase model complexity**: Experimenting with more complex CNN architectures could result in a better ability to capture discriminative features within neonatal 3D MRI data. This could involve increasing the depth of the network by adding more convolutional and fully connected layers and increasing the number of neurons for the fully connected layers or experimenting with different type of layers and activation functions.
- **Experiment with functional MRI**: Training a CNN model on 4D brain fMRI or integrating both structural and functional MRI data into a single model could provide richer information for the CNN to learn from and potentially improving its prediction capabilities.
- **Experiment with different datasets**: Using larger and better distributed datasets could help in achieving better model's performance and better generalisability of the findings.

- **Use other metrics**: Exploring other relevant metrics or outcomes that could be predicted from neonatal MRI data other than Q-CHAT scores could expand the applicability of the model beyond autism risk assessment.

This project discovers a new potential in neonatal brain MRI data analysis and recommends further exploration and refinement of the methodologies used, with the ultimate goal of improving early detection and intervention strategies for neurodevelopmental conditions, such as ASD.

Reference List

1. Abraham, A. *et al.* (2017) 'Deriving reproducible biomarkers from multi-site resting-state data: An Autism-based example', *NeuroImage*, 147, pp. 736–745. Available at: https://doi.org/10.1016/j.neuroimage.2016.10.045.
2. Aghdam, M.A., Sharifi, A. and Pedram, M.M. (2019) 'Diagnosis of Autism Spectrum Disorders in Young Children Based on Resting-State Functional Magnetic Resonance Imaging Data Using Convolutional Neural Networks', *Journal of Digital Imaging*, 32(6), pp. 899–918. Available at: https://doi.org/10.1007/s10278-019-00196-1.
3. Allison, C. *et al.* (2021) 'Quantitative Checklist for Autism in Toddlers (Q-CHAT). A population screening study with follow-up: the case for multiple time-point screening for autism', *BMJ Paediatrics Open*, 5(1), p. e000700. Available at: https://doi.org/10.1136/bmjpo-2020-000700.
4. Anderson, A. (no date) *GitHub - ScytheNight/Loop-Over-Files-Bash: Loops over files in bash.* Available at: https://github.com/ScytheNight/Loop-Over-Files-Bash (Accessed: 20 May 2024).
5. Batalle, D. *et al.* (no date) *CoDe Neuro Lab*, *CoDe Neuro Lab*. Available at: https://www.code-neuro.com/ (Accessed: 20 May 2024).
6. CDC (2022) *Diagnostic Criteria | Autism Spectrum Disorder (ASD) | NCBDDD | CDC*, *Centers for Disease Control and Prevention*. Available at: https://www.cdc.gov/ncbddd/autism/hcp-dsm.html (Accessed: 1 February 2024).
7. CDC (2024) *Data and Statistics on Autism Spectrum Disorder | CDC*, *Centers for Disease Control and Prevention*. Available at: https://www.cdc.gov/ncbddd/autism/data.html (Accessed: 1 February 2024).
8. Chen, R., Jiao, Y. and Herskovits, E.H. (2011) 'Structural MRI in Autism Spectrum Disorder', *Pediatric Research*, 69(8), pp. 63–68. Available at: https://doi.org/10.1203/PDR.0b013e318212c2b3.
9. Corballis, M.C. (2014) 'Left Brain, Right Brain: Facts and Fantasies', *PLoS Biology*, 12(1), p. e1001767. Available at: https://doi.org/10.1371/journal.pbio.1001767.
10. Edwards, A.D. *et al.* (2022) 'The Developing Human Connectome Project Neonatal Data Release', *Frontiers in Neuroscience*, 16, p. 886772. Available at: https://doi.org/10.3389/fnins.2022.886772.
11. El-Baba, R.M. and Schury, M.P. (2024) 'Neuroanatomy, Frontal Cortex', in *StatPearls*. Treasure Island (FL): StatPearls Publishing. Available at: http://www.ncbi.nlm.nih.gov/books/NBK554483/ (Accessed: 17 March 2024).
12. França, L.G.S. *et al.* (2024) 'Neonatal brain dynamic functional connectivity in term and preterm infants and its association with early childhood neurodevelopment', *Nature Communications*, 15(1), p. 16. Available at: https://doi.org/10.1038/s41467-023-44050-z.
13. *FreeSurfer* (no date) *FreeSurfer*. Available at: https://surfer.nmr.mgh.harvard.edu (Accessed: 4 May 2024).
14. Giedd, J.N. (2004) 'Structural Magnetic Resonance Imaging of the Adolescent Brain', *Annals of the New York Academy of Sciences*, 1021(1), pp. 77–85. Available at: https://doi.org/10.1196/annals.1308.009.
15. Heeger, D.J. and Ress, D. (2002) 'What does fMRI tell us about neuronal activity?', *Nature Reviews Neuroscience*, 3(2), pp. 142–151. Available at: https://doi.org/10.1038/nrn730.

16. Helmy, E. *et al.* (2023) 'Role of Artificial Intelligence for Autism Diagnosis Using DTI and fMRI: A Survey', *Biomedicines*, 11(7), p. 1858. Available at: https://doi.org/10.3390/biomedicines11071858.
17. Herlin, B., Navarro, V. and Dupont, S. (2021) 'The temporal pole: From anatomy to function—A literature appraisal', *Journal of Chemical Neuroanatomy*, 113, p. 101925. Available at: https://doi.org/10.1016/j.jchemneu.2021.101925.
18. *ImageNet* (no date). Available at: https://www.image-net.org/about.php (Accessed: 10 May 2024).
19. Jain, S. *et al.* (2023) 'Autism Detection of MRI Brain Images Using Hybrid Deep CNN With DM-Resnet Classifier', *IEEE Access*, 11, pp. 117741–117751. Available at: https://doi.org/10.1109/ACCESS.2023.3325701.
20. Johnson, K.A. and Becker, A.J. (1995) *The Whole Brain Atlas*. Available at: https://www.med.harvard.edu/aanlib/cases/caseM/mr1_t/032.html (Accessed: 2 March 2024).
21. Katuwal, G.J. *et al.* (2016) 'Divide and Conquer: Sub-Grouping of ASD Improves ASD Detection Based on Brain Morphometry', *PLOS ONE*, 11(4), p. e0153331. Available at: https://doi.org/10.1371/journal.pone.0153331.
22. Leech, R. and Sharp, D.J. (2014) 'The role of the posterior cingulate cortex in cognition and disease', *Brain*, 137(1), pp. 12–32. Available at: https://doi.org/10.1093/brain/awt162.
23. Lord, C. *et al.* (2018) 'Autism spectrum disorder', *The Lancet*, 392(10146), pp. 508–520. Available at: https://doi.org/10.1016/S0140-6736(18)31129-2.
24. Makropoulos, A. *et al.* (2018) 'The developing human connectome project: A minimal processing pipeline for neonatal cortical surface reconstruction', *NeuroImage*, 173, pp. 88–112. Available at: https://doi.org/10.1016/j.neuroimage.2018.01.054.
25. McCarty, P. and Frye, R.E. (2020) 'Early Detection and Diagnosis of Autism Spectrum Disorder: Why Is It So Difficult?', *Seminars in Pediatric Neurology*, 35, p. 100831. Available at: https://doi.org/10.1016/j.spen.2020.100831.
26. McGrath, H. *et al.* (2022) 'High-resolution cortical parcellation based on conserved brain landmarks for localization of multimodal data to the nearest centimeter', *Scientific Reports*, 12(1), p. 18778. Available at: https://doi.org/10.1038/s41598-022-21543-3.
27. Mercadante, A.A. and Tadi, P. (2024) 'Neuroanatomy, Gray Matter', in *StatPearls*. Treasure Island (FL): StatPearls Publishing. Available at: http://www.ncbi.nlm.nih.gov/books/NBK553239/ (Accessed: 17 March 2024).
28. Nogay, H.S. and Adeli, H. (2020) 'Machine learning (ML) for the diagnosis of autism spectrum disorder (ASD) using brain imaging', *Reviews in the Neurosciences*, 31(8), pp. 825–841. Available at: https://doi.org/10.1515/revneuro-2020-0043.
29. Okoye, C. *et al.* (2023) 'Early Diagnosis of Autism Spectrum Disorder: A Review and Analysis of the Risks and Benefits', *Cureus*, 15(8), p. e43226. Available at: https://doi.org/10.7759/cureus.43226.
30. Padmanaban, S. *et al.* (2020) 'A Role of Medical Imaging Techniques in Human Brain Tumor Treatment', 8, pp. 565–568. Available at: https://doi.org/10.35940/ijrte.D1105.1284S219.
31. Pereira, A.M. *et al.* (2018) 'Differences in Cortical Structure and Functional MRI Connectivity in High Functioning Autism', *Frontiers in Neurology*, 9. Available at:

https://www.frontiersin.org/journals/neurology/articles/10.3389/fneur.2018.00539 (Accessed: 17 February 2024).
32. Power, J.D. *et al.* (2017) 'Sources and implications of whole-brain fMRI signals in humans', *NeuroImage*, 146, pp. 609–625. Available at: https://doi.org/10.1016/j.neuroimage.2016.09.038.
33. Pykes, C. (2023) *PyTorch vs TensorFlow vs Keras for Deep Learning: A Comparative Guide*. Available at: https://www.datacamp.com/tutorial/pytorch-vs-tensorflow-vs-keras (Accessed: 3 May 2024).
34. *Quantitative Checklist for Autism in Toddlers (Q-CHAT)* (2008) *Psychology Tools*. Available at: https://psychology-tools.com/qchat-quantitative-checklist-for-autism-in-toddlers/ (Accessed: 1 May 2024).
35. Rafiee, F. *et al.* (2022) 'Brain MRI in Autism Spectrum Disorder: Narrative Review and Recent Advances', *Journal of Magnetic Resonance Imaging*, 55(6), pp. 1613–1624. Available at: https://doi.org/10.1002/jmri.27949.
36. Rahman, M.M. *et al.* (2020) 'A Review of Machine Learning Methods of Feature Selection and Classification for Autism Spectrum Disorder', *Brain Sciences*, 10(12), p. 949. Available at: https://doi.org/10.3390/brainsci10120949.
37. *ResNet* (no date) *PyTorch*. Available at: https://pytorch.org/hub/pytorch_vision_resnet/ (Accessed: 8 May 2024).
38. Rogers, B.P. *et al.* (2007) 'Assessing functional connectivity in the human brain by fMRI', *Magnetic Resonance Imaging*, 25(10), pp. 1347–1357. Available at: https://doi.org/10.1016/j.mri.2007.03.007.
39. Segovia, F. *et al.* (2014) 'Identifying endophenotypes of autism: a multivariate approach', *Frontiers in Computational Neuroscience*, 8. Available at: https://www.frontiersin.org/articles/10.3389/fncom.2014.00060 (Accessed: 24 February 2024).
40. Selcuk Nogay, H. and Adeli, H. (2023) 'Diagnostic of autism spectrum disorder based on structural brain MRI images using, grid search optimization, and convolutional neural networks', *Biomedical Signal Processing and Control*, 79, p. 104234. Available at: https://doi.org/10.1016/j.bspc.2022.104234.
41. Sharma, R., Sekhon, S. and Cascella, M. (2024) 'White Matter Lesions', in *StatPearls*. Treasure Island (FL): StatPearls Publishing. Available at: http://www.ncbi.nlm.nih.gov/books/NBK562167/ (Accessed: 17 March 2024).
42. Srimal, A. *et al.* (2019) *Topological inference from spontaneous activity structures in FMRI videos with peristence barcodes*. Available at: https://doi.org/10.1101/809293.
43. Symms, M. *et al.* (2004) 'A review of structural magnetic resonance neuroimaging', *Journal of Neurology, Neurosurgery & Psychiatry*, 75(9), pp. 1235–1244. Available at: https://doi.org/10.1136/jnnp.2003.032714.
44. Thompson, P.M. *et al.* (2005) 'Structural MRI and Brain Development', in *International Review of Neurobiology*. Academic Press (Neuroimaging, Part B), pp. 285–323. Available at: https://doi.org/10.1016/S0074-7742(05)67009-2.
45. Wang, Z. and Bovik, A.C. (2009) 'Mean squared error: Love it or leave it? A new look at Signal Fidelity Measures', *IEEE Signal Processing Magazine*, 26(1), pp. 98–117. Available at: https://doi.org/10.1109/MSP.2008.930649.
46. 'WMA - The World Medical Association-WMA Declaration of Helsinki – Ethical Principles for Medical Research Involving Human Subjects' (no date). Available at:

https://www.wma.net/policies-post/wma-declaration-of-helsinki-ethical-principles-for-medical-research-involving-human-subjects/ (Accessed: 14 May 2024).
47. Xu, M. *et al.* (2021) 'Brain imaging-based machine learning in autism spectrum disorder: methods and applications', *Journal of Neuroscience Methods*, 361, p. 109271. Available at: https://doi.org/10.1016/j.jneumeth.2021.109271.
48. Zafar, A. (2023) 'TensorFlow vs. PyTorch vs. Keras vs. Scikit: A Comprehensive Comparison', *Medium*, 19 October. Available at: https://aqsazafar81.medium.com/tensorflow-vs-pytorch-vs-keras-vs-scikit-a-comprehensive-comparison-81c620298f00 (Accessed: 3 May 2024).
49. Zeidman, P. and Maguire, E.A. (2016) 'Anterior hippocampus: the anatomy of perception, imagination and episodic memory', *Nature reviews. Neuroscience*, 17(3), pp. 173–182. Available at: https://doi.org/10.1038/nrn.2015.24.
50. Zhao, Y. *et al.* (2018) '3D Deep Convolutional Neural Network Revealed the Value of Brain Network Overlap in Differentiating Autism Spectrum Disorder from Healthy Controls', in A.F. Frangi et al. (eds) *Medical Image Computing and Computer Assisted Intervention – MICCAI 2018*. Cham: Springer International Publishing (Lecture Notes in Computer Science), pp. 172–180. Available at: https://doi.org/10.1007/978-3-030-00931-1_20.

Appendices

Appendix 1: Terms of Reference

KV6003: Individual Computing Project Terms of References	
Student name:	Filip Kovarik
Student ID:	20010297
Course:	BSc (Hons) Computer Science
Project title:	The interplay between neonatal brain structure and function in neurodevelopment.
Supervisor:	Dr. Lucas França
2nd Marker:	Shanfeng Hu

Guidance for each section is included under each heading, but more detail can be found in the module Handbook.

1. Background to Project

This project will investigate associations between the neonatal brain structure on its function and associate the findings with relevant clinical markers. The investigation will be conducted on a dataset of structural magnetic resonance imagery (MRI) and functional MRI scans taken from neonates in the context of the developing Human Connectome Project (dHCP). Appropriate machine learning tools will be used to analyse patterns between the two types of MRI scans and trained for predicting clinical features which are linked to neurodevelopment in later stages of the neonate's life.

The project's domain is computational neuroscience, which could be defined as an interplay of neural data, computation, and applied mathematics. It is the problem area in which algorithmic or implementational questions are closely related to data of a nervous system (Schwartz, 1990).

My initial idea was to use machine learning methods to aid in healthcare related questions, which eventually formed into the current project's topic, which aligns and builds upon the supervisor's research area. Existing literature primarily investigates applying machine learning strategies on various types of MRI to identify a single specific brain condition, as shown in a report by Helmy et al. (2023). Exploring the developing neonatal brain using MRI is still a relatively new area with a lot of research opportunities. There is also a lack of literature investigating the interplay of structural and functional MRI scans might have on a neonatal brain, which is the focus of this project.

Working on this project will involve understanding relevant neuroscientific literature, learning to work with new tools for visualizing and analyzing brain imaging data and

implementing a machine learning model to understand potential connections of the two types of MRI scans.

2. Proposed Work

The development pipeline of this project will involve data pre-processing (normalization, motion correction…), feature extraction and selection, training a neural network model on the pre-processed MRI data, and finally, an evaluation of the model's performance and results. A critical part of the process will be finding a neural network algorithm which achieves best results. For example, recent literature dominantly uses convolutional neural networks (CNNs) for brain MRI regression or classification (Korolev *et al.*, 2017; Sarraf *et al.*, 2017; Ariyarathne *et al.*, 2020; Bakr Siddique *et al.*, 2020). The reason for that is CNN enables autonomous feature selection and is powerful in computer vision related problems even with smaller datasets.

As a result, I expect to identify relationships between structural and functional changes in a neonatal brain which could be associated with relevant clinical features.

The preparatory part of this project will therefore require an extensive literature review looking into:

- How MRI works and what information can be learned from analyzing MRI scans of the brain,
- the state-of-the-art tools and machine learning techniques used to analyze MRI scans and how to use those to detect abnormalities in the brain,
- investigating the challenges of MRI scans taken on neonatal brains and how the analyzing strategy might differ from scans taken on the adult brain.

This will help me understand and work with this type of neuroimaging data. The practical part will involve working with a dataset of structural and functional MRI scans of neonatal brains acquired from the developing human connectome project (dHCP). To carry out the practical part, the Python programming language is suggested to be used along with relevant libraries, such as scikit-learn and MNE-Python. Acquiring the relevant skills needed for using these tools will also be a part of the project work.

3. Aims of Project

The project's aim is to investigate and analyse possible patterns of how the neonatal brain's structure might be linked to its function by training a machine learning model to identify changes in neuroimaging data which might be linked to neurodevelopment.

4. Objectives

- Review recent literature presenting how AI is used in brain's MRI analysis and how is this different in adult vs. neonatal brain,
- Identify the optimal approach/methodology for the study,
- Acquire the necessary skills required for using Python and relevant libraries (MNE-Python, scikit-learn…),
- Train a machine learning model using the provided dataset,
- Fine-tune and optimise the model for best performance,
- Evaluate and analyse the model's findings,
- Produce a detailed documentation for the project's practical part,
- Discuss the findings and give proposal for future work.

5. Skills

SKILL	KNOWLEDGE DEGREE (NONE, LOW, INTERMEDIATE, HIGH)	ACQUIRED / WILL ACQUIRE FROM
UNDERSTANDING OF MRI DATA	None	Literature, supervisor guidance
MACHINE LEARNING THEORY	Intermediate	KF5042, KF6052
PYTHON	Intermediate	Self-learned
MNE-PYTHON	None	Official documentation, supervisor guidance
SCIKIT-LEARN	Low	Self-learning, need to improve – official documentation

6. Sources of information / bibliography

Schwartz, E.L. (1990). *Computational Neuroscience*. [online] Cambridge, Mass.: Mit Press. Available at: https://www.google.co.uk/books/edition/Computational_Neuroscience/LZ4sBy0kyRoC?hl=en&gbpv=0 [Accessed 21 Oct. 2023].

Helmy, E., Elnakib, A., Yaser ElNakieb, Khudri, M., Abdelrahim, M., Yousaf, J., Ghazal, M., Contractor, S., Gregory Neal Barnes and El-Baz, A.S. (2023). Role of Artificial Intelligence for

Autism Diagnosis Using DTI and fMRI: A Survey. *Biomedicines*, [online] 11(7), pp.1858–1858. doi:https://doi.org/10.3390/biomedicines11071858.

Ariyarathne, G. *et al.* (2020) 'ADHD Identification using Convolutional Neural Network with Seed-based Approach for fMRI Data', in *Proceedings of the 2020 9th International Conference on Software and Computer Applications*. New York, NY, USA: Association for Computing Machinery (ICSCA '20), pp. 31–35. Available at: https://doi.org/10.1145/3384544.3384552.
Bakr Siddique, Md.A. *et al.* (2020) 'Deep Convolutional Neural Networks Model-based Brain Tumor Detection in Brain MRI Images', in *2020 Fourth International Conference on I-SMAC (IoT in Social, Mobile, Analytics and Cloud) (I-SMAC)*. *2020 Fourth International Conference on I-SMAC (IoT in Social, Mobile, Analytics and Cloud) (I-SMAC)*, pp. 909–914. Available at: https://doi.org/10.1109/I-SMAC49090.2020.9243461.
Korolev, S. *et al.* (2017) 'Residual and plain convolutional neural networks for 3D brain MRI classification', in *2017 IEEE 14th International Symposium on Biomedical Imaging (ISBI 2017)*. *2017 IEEE 14th International Symposium on Biomedical Imaging (ISBI 2017)*, pp. 835–838. Available at: https://doi.org/10.1109/ISBI.2017.7950647.
Sarraf, S. *et al.* (2017) 'DeepAD: Alzheimer's Disease Classification via Deep Convolutional Neural Networks using MRI and fMRI'. bioRxiv, p. 070441. Available at: https://doi.org/10.1101/070441.
The Developing Human Connectome Project (no date). Available at: http://www.developingconnectome.org/ (Accessed: 1 November 2023).

7. Resources - statement of hardware / software required

- Software / development tools – Python, MNE-Python, Scikit-learn (these are all free to use)
- Hardware – Access to a university's high-performance computer for training the model

8. Assessment criteria for practical computing work

Dissertation (60%):
- Abstract – 5%
- Introduction – 10%
- Literature Review, Research and Planning – 60%
- Evaluation – 20%
- Conclusions and Recommendations – 5%

Practical Work (40%):
- Methods – 40%
- Results and Discussion – 50%
- Quality of Code – 10%

9. Ethics, Social, Legal and Professional Issues

This project is considered low risk in the ethics, social, legal, and professional issues question. A separate ethics form has been submitted.

10. Project Plan - Schedule of activities

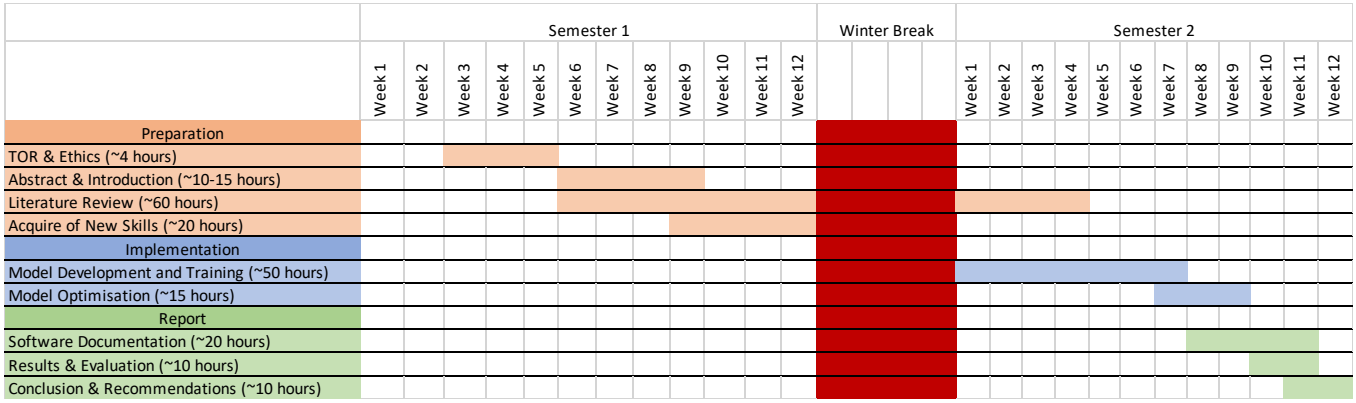

Appendix 2: Ethics Approval Form

Student Name:	Filip Kovarik
Student ID:	20010297
Programme Name (e.g. BSc Computer Science, BSc Computer Networks and Cyber Security):	BSc (Hons) Computer Science
Project Title:	The interplay between neonatal brain structure and function
Supervisor Name:	Lucas França
Second Marker:	Shanfeng Hu
What type of study are you using (check all that apply):	☐ Questionnaire or Survey ☐ User Studies ☐ Data Generated by Systems ☒ Secondary Data Analysis ☐ No data collected from humans

Please answer the following questions and complete all information in full:

1. **Human Participants**: does your study involve human participants ~~YES~~/NO

If ***YES***, please answer the following questions and ensure that you include your participant information sheet, participant consent sheet and any participant recruitment materials/permission letters for participants in Appendix B:

1a) Who are your participants and what is the inclusion criteria you will be using?	
1b) How many participants will you recruit and from where?	
1c) Are there any exclusion criteria (reasons why people should not participate)?	

2. **Data Collection:** Will your study collect any primary data or use any secondary data not in the public domain? YES/~~NO~~

Please complete the following questions, noting that somebody should be able to read this and replicate your approach:

2a) What type of data are you going to use? (Identify main types of information/data)	MRI scans of neonatal brains acquired from developing Human Connectome Project (dHCP).
2b) What procedures will you use to collect data (include all equipment/methods you plan to use)	-
2c) What methods will you use to analyse this data?	Visualizing and machine learning tools in Python

3. Data Management

Standard phrases have been added to the information sheet (available on Blackboard). In rare instances, these may not be appropriate for your study. If not, please describe any additional data management procedures below:

All data will be stored on the University's OneDrive network and where appropriate additionally protected with a password. The results will be used for an undergraduate project that will be examined as part of BSc (Hons) Computer Science degree. Occasionally some results might be presented at a conference or published in a journal, but they will always remain anonymous. All data used in this project will be secondary data and will be stored in line with the General Data Protection Regulation (GDPR).

4. Risk Assessment, Health and Safety

All research activity carried out by Northumbria University is subject to risk assessment and health and safety issues. Depending on the nature of your research work, you may need to use one of the risk assessments below and/or complete a Project Risk Assessment in discussion with your supervisor. Once you have identified risks and associated health and safety issues, you may need to consult relevant technical and other staff for further advice and guidance. Further information including a blank risk assessment form for research can be found here: Risk Assessment (northumbria.ac.uk).

Please check this box after you have read and understood ethics and health and safety information

☒ I confirm I have read the University's health and safety policy and ethics policy. I have read and understood the requirement for the mandatory completion of risk assessments and that my study does not deviate from the module level approval ethics information on Blackboard**:** *Relevant risk assessments are listed in the ethics application. If your project needs additional risk assessments, then you will need to submit a new ethics application. Please identify the elements of the listed risk assessment that are relevant for your study and the risk assessment(s) you are working with. Note that these are only relevant if you are collecting data face-to-face.*

Please check the relevant boxes:

☒ No physical risks

☐ HL_RISK_173 Testing in an external environment

☐ HL_RISK_722 Face-to-face interview

☐ HL_RISK_727 Group interview

Supervisor (and/or Second Marker where appropriate) to assess using the following criteria:

Tutor sign off	
Ethics form complete	☐
Ethical concerns acknowledged	☐
Research tool(s) checked	☐

All relevant forms included (consent etc.)	☐
Is not high risk	☐

Appendix 3: Training data for the pre-trained 2D CNN model

Epoch	Average training loss	Average validation loss
1	133.6805	89.2023
2	99.9914	162.8961
3	100.1500	134.3488
4	98.7321	122.1435
5	98.5028	170.1278
6	99.1628	174.0568

Appendix 4: Training data for the custom 3D CNN model

Epoch	Average training loss	Average validation loss
1	18134273.8076	1593.1600
2	2271.0497	1053.3151
3	1043.3382	961.5066
4	930.1174	863.5981
5	863.1431	770.9316
6	763.2549	680.3120
7	965.6540	586.9765
8	569.4957	509.2319
9	486.1337	437.8982
10	418.7354	372.7618
11	367.6659	318.1154
12	322.8996	269.8849
13	268.8642	224.8377
14	226.4553	198.4819
15	206.0293	172.3874
16	186.5644	144.6348
17	158.4290	134.0468
18	140.0603	120.9631
19	135.9430	114.2352
20	134.7753	108.9150
21	115.2497	104.1605
22	114.9782	104.5679
23	124.9838	101.3686
24	116.9430	103.1706
25	113.5447	102.8630
26	108.9903	102.2019
27	121.9602	102.4849
28	112.4003	101.6834

Appendix 5: Training data for the custom 3D CNN model after oversampling

Epoch	Average training loss	Average validation loss
1	18456321.2302	1035.8013
2	1741.2186	967.6056
3	1228.7888	924.1528
4	1005.4217	832.4914
5	1023.6926	851.6757
6	1080.4502	695.6945
7	818.4890	580.9106
8	787.6853	522.3470
9	677.3490	525.8318
10	585.0487	441.5229
11	683.4710	404.0059
12	522.4496	348.5814
13	474.4731	314.5345
14	479.3048	290.8568
15	449.4357	251.4505
16	337.0757	221.7104
17	326.0189	206.5856
18	288.8558	179.9238
19	280.8382	154.4115
20	276.5111	163.7426
21	262.0919	144.7463
22	267.1083	132.7621
23	249.7636	114.9986
24	257.5160	136.2729
25	259.6227	123.9444
26	229.6136	127.1790
27	231.1568	122.4737
28	236.6919	135.5030